

Kinetics and Products of the Self-Reaction of Propargyl Radicals

Eugene V. Shafir, Irene R. Slagle, and Vadim D. Knyazev*

Research Center for Chemical Kinetics, Department of Chemistry, The Catholic University of America, Washington, DC 20064

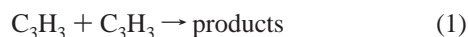
Received: June 10, 2003; In Final Form: August 6, 2003

The kinetics and product branching of the self-reaction of propargyl radicals, $C_3H_3 + C_3H_3 \rightarrow$ products (1), have been studied as functions of temperature. Rate constants of reaction 1 were obtained in direct real-time experiments by laser photolysis/photoionization mass spectrometry over the temperature interval 500–1000 K and at a bath gas density of $(3-6) \times 10^{16}$ molecules cm^{-3} . Propargyl radicals were produced by the 248 nm laser photolysis of oxalyl chloride ((CClO)₂) followed by a fast conversion of the produced chlorine atoms into propargyl radicals and HCl via the reaction with propyne. No active species other than C_3H_3 were present in the system during the kinetics of C_3H_3 decay. The values of the rate constant of reaction 1 were determined from the $[C_3H_3]$ temporal profiles. The rate constants of reaction 1 decrease from $(3.30 \pm 0.35) \times 10^{-11}$ cm^3 molecule⁻¹ s⁻¹ at 500 K to $(2.74 \pm 0.43) \times 10^{-11}$ cm^3 molecule⁻¹ s⁻¹ at 700 K and to $(1.20 \pm 0.14) \times 10^{-11}$ cm^3 molecule⁻¹ s⁻¹ at 1000 K. The value obtained at 1000 K is likely to be influenced by falloff effects and secondary reactions initiated by the $H + C_6H_5$ products of reaction 1. The rate constants of reaction 1 determined in the current study at elevated temperatures correlate well with the room temperature value of $\sim 4 \times 10^{-11}$ cm^3 molecule⁻¹ s⁻¹ obtained in several earlier studies. Combination of the results of the current work with those of earlier room temperature investigations results in the following temperature dependence of the high-pressure-limit rate constant of reaction 1: $k_1^\infty = 4.49 \times 10^{-9} T^{-0.75} \exp(-128 K/T)$ cm^3 molecule⁻¹ s⁻¹ (295–700 K). Product channels of reaction 1 were studied using final product analysis by gas chromatography/mass spectrometry in the 500–1100 K temperature interval. Several C_6H_6 isomers were detected as products of the self-reaction of propargyl radicals: 1,5-hexadiyne, fulvene, benzene, and two unknown species identified in the text as unknown 1 and unknown 2. The distribution of products depends on the temperature. At lower temperatures, 1,5-hexadiyne, unknown 1, and benzene were observed. The fraction of benzene increases with temperature; it becomes the major product at 900 K and above. Fulvene and unknown 2 were observed in minor amounts in the 900–1100 K range. The product analysis provides evidence for the appearance of the reaction channel 1b ($C_6H_5 + H$) at high temperatures: formation of C_8H_6 and C_9H_8 was observed and attributed to the fast reaction of the phenyl radical with the excess of propyne present in the reactor.

I. Introduction

Formation of polycyclic aromatic hydrocarbons (PAH) has been long recognized as an important step in the production of soot in the combustion of hydrocarbon fuels. Numerous efforts have been concentrated on the elucidation of chemical pathways leading to the formation of the first aromatic ring.¹ In a number of publications, the recombination of propargyl radicals followed by isomerization of the adduct has been identified as a likely pathway leading to the formation of benzene.^{2–8} Propargyl radicals are present in many types of flames in high concentrations due to their low reactivity toward molecular oxygen,⁹ which facilitates their self-reaction as well as reaction with other species present in high concentrations.

Over the past 15 years, a number of experimental studies of the propargyl radical self-reaction has been published (refs 4, 5, 10–13):



Alkemade and Homann⁴ studied reaction 1 at temperatures 623–

673 K. Propargyl radicals were generated by the reaction between sodium vapor and propynyl halides (C_3H_3Cl or C_3H_3Br) in a low-pressure flow reactor by a multislit burner and detected by mass spectrometry. The authors derived a value of 5.6×10^{-11} cm^3 molecule⁻¹ s⁻¹ for the rate constant of reaction 1 from kinetic simulation of the observed profile of the C_6H_6 product. In a later work, Morter et al.¹⁰ obtained the value of $k_1 = (1.2 \pm 0.2) \times 10^{-10}$ cm^3 molecule⁻¹ s⁻¹ at 295 K using the technique of laser photolysis/infrared absorption spectroscopy; photolysis of C_3H_3Cl and C_3H_3Br was used as a source of propargyl radicals. Two studies by Fahr and Nayak⁵ and by Atkinson and Hudgens¹¹ found the rate constant of the propargyl radical self-reaction to be approximately 3 times lower, $(4.3 \pm 0.6) \times 10^{-11}$ (at 295 K) and $(4.0 \pm 0.4) \times 10^{-11}$ cm^3 molecule⁻¹ s⁻¹ (at 298 K), respectively, in agreement with each other. Fahr and Nayak used laser photolysis of propargyl chloride with gas chromatography/mass spectrometry; the value of k_1 was derived from kinetic modeling based on the experimental product yields and literature data on the rate constants of other reactions involved. Atkinson and Hudgens employed UV cavity ring-down spectroscopy with laser photolysis of allene, propargyl chloride, and propargyl bromide. A recent room temperature

* Corresponding author: e-mail knyazev@cua.edu.

study of DeSain and Taatjes¹³ produced $k_1 = (3.9 \pm 0.6) \times 10^{-11} \text{ cm}^3 \text{ molecule}^{-1} \text{ s}^{-1}$, in agreement with the values of refs 5 and 11. A high temperature (1100–2100 K) value of the propargyl radical self-reaction rate constant was estimated to be between 7.5×10^{-12} and $1.5 \times 10^{-11} \text{ cm}^3 \text{ molecule}^{-1} \text{ s}^{-1}$ in the shock-tube experiments of Scherer et al.¹² using 3-iodopropyne as the source of propargyl radicals.

Products of reaction 1 have been reported in ref 4 (623–673 K) and ref 5 (room temperature). Two more experimental studies of the kinetics¹⁴ and products¹⁵ of reaction 1 are currently being finalized.

Theoretical studies of the $\text{C}_3\text{H}_3 + \text{C}_3\text{H}_3$ reaction include works by Miller and Melius⁷ and Melius et al.⁸ on the potential energy surface (PES) and by Miller and Klippenstein¹⁶ on the solution of the master equation and evaluation of the temperature and pressure dependences of the rate constant and the distribution of products. A recent study of Miller and Klippenstein¹⁷ combined a new investigation of the reaction PES with a master equation study of the kinetics and products.

In the current article we present the results of an experimental investigation of the kinetics and products of the self-reaction of propargyl radicals as functions of temperature.¹⁸ The kinetics of reaction 1 was studied by laser photolysis/photoionization mass spectrometry. A relatively novel approach was used to create propargyl radicals employing a reaction between Cl atoms obtained by photolysis of oxalyl chloride^{19,20} with propyne.²¹ This approach results in a well-defined initial concentration of C_3H_3 with no other active species present in the reactor during the kinetics of the C_3H_3 decay. Overall rate constants were obtained in the temperature interval 500–1000 K and at bath gas (mostly He, balance radical precursors) densities of $(3\text{--}6) \times 10^{16} \text{ molecules cm}^{-3}$. Product channels of reaction 1 were studied using final product analysis by gas chromatography/mass spectrometry.

This article is organized as follows. Section I is an introduction. Section II presents the experimental methods used for determination of the rate constants and for the product analysis. Experimental results are presented in section III followed by a discussion in section IV. Conclusions are given in section V.

II. Experimental Methods

In this section a description of the experimental apparatus used in the kinetic study and the choice of the photolytic source of radicals are first presented. Next, the method of determination of the rate constants is described. Finally, a description of the apparatus and the method employed for the product analysis is given.

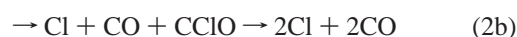
Kinetic Apparatus. Details of the experimental apparatus have been described previously;²² only a brief description is given here. Pulsed 248 nm unfocused light from a Lambda Physik 201 MSC excimer laser was directed along the axis of a heated 50 cm long tubular quartz reactor (i.d. 1.05 cm). The reactor surface was coated with boron oxide to reduce radical wall losses.²³ The laser was operated at a frequency of 3 Hz and a fluence of 150–400 mJ pulse⁻¹.

To replace the photolyzed gas mixture with fresh reactants between laser pulses, the flow of the gas mixture containing the radical precursors and the bath gas (helium) was set at $\approx 4 \text{ m s}^{-1}$. The mixture was continuously sampled through a small tapered orifice in the wall of the reactor and formed into a beam by a conical skimmer before entering the vacuum chamber containing the photoionization mass spectrometer. As the gas beam traversed the ion source, a portion was photoionized by an atomic resonance lamp, mass selected by a quadrupole mass

filter, and detected by a Daly detector.³⁶ Temporal ion signal profiles were recorded from a short time before the laser pulse (10–30 ms) to 15–30 ms following the pulse by a multichannel scaler. Typically, data from 1000 to 15 000 repetitions of the experiment were accumulated before the data were analyzed. The sources of the photoionization radiation were chlorine (8.9–9.1 eV, CaF_2 window, used to detect C_3H_3 at 1000 K and C_2H_5), hydrogen (10.2 eV, MgF_2 window, used to detect C_6H_6 , C_8H_6 , C_9H_8 , $\text{C}_3\text{H}_4\text{Cl}$, and C_3H_3 at 500 and 700 K), and neon (16 eV, collimated hole structure, used to detect HCl and $(\text{CClO})_2$ resonance lamps).

Radical Precursors. Real-time experimental studies of radical self-reactions, ideally, require a suitable pulsed source of radicals that should satisfy two requirements: (1) that the radicals of interest are the only reactive species present in the reactor during the kinetics of radical decay and (2) that the initial concentration of radicals can be determined with a high degree of accuracy.

Recently, Baklanov and Krasnoperov¹⁹ suggested using the 193 nm photolysis of oxalyl chloride $(\text{CClO})_2$ with consecutive conversion of Cl atoms to radicals of interest (R) and HCl by a fast reaction with a suitable substrate:



The 193 nm photolysis of oxalyl chloride can serve as a “clean” photolytic source of chlorine atoms (“clean” in the sense that no other reactive species are produced by the photolysis). Since the yield of chlorine atoms in reaction 2 is exactly 200%, the initial concentration of Cl (and, consequently, that of R) can be determined from the extent of the photolytic depletion of oxalyl chloride, which, in turn, can be measured spectroscopically²⁰ or mass spectrometrically. Baklanov and Krasnoperov used this method of pulsed generation of radicals to study the self-reaction of silyl radicals.²⁰ Recently, we have applied the method of Baklanov and Krasnoperov (reactions 2 and 3) to the study of the ethyl radical self-reaction.²⁴ The initial concentration of the radicals can also be determined by measuring the production of HCl since HCl and the radicals of interest are produced in reaction 3 in a 1:1 ratio. The equivalence of the two methods of evaluating the initial concentration of Cl and R was verified in a separate set of experiments. The concentration of ethyl radicals obtained in the reaction between the chlorine atoms produced in the photolysis of oxalyl chloride with ethane was determined by measuring (1) the production of HCl and (2) the photolytic depletion of $(\text{CClO})_2$ in the 193 nm photolysis of oxalyl chloride over a 300–900 K range of temperatures. The values obtained by these two different methods were found to be equal within experimental uncertainties. Measured flows of (gaseous) HCl were used for calibration of the HCl ion signal.

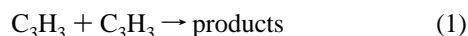
In the experiments on the kinetics of reaction 1, the photolysis of $(\text{CClO})_2$ followed by the subsequent fast reaction of the Cl atoms with propyne was used as a source of propargyl radicals. To avoid interference from the photodissociation of propyne,¹¹ 248 nm (instead of 193 nm) photolysis was used. It is safe to assume that the 248 nm photolysis of $(\text{CClO})_2$ produces the same products as the 193 nm²⁵ or 235 nm²⁶ photolysis, since the CClO radical has a high thermal decomposition rate at temperatures of 500 K and above (e.g., $k > 10^4 \text{ s}^{-1}$ at the pressures used in the current study, as estimated from the results

of ref 27). Since the 248 nm photolysis of $(\text{CClO})_2$ is less efficient than the 193 nm photolysis, higher concentrations of oxalyl chloride had to be used, and measurement of the photolytic depletion of $(\text{CClO})_2$ became impractical due to the low values of the fraction of oxalyl chloride decomposed due to photolysis. Thus, production of HCl was used to determine the initial concentrations of C_3H_3 . Concentrations of propyne were selected to ensure a virtually instantaneous (on the time scale of the reactions studied) conversion of Cl into the radicals of interest, C_3H_3 , and HCl. The rate of the reverse reaction, that of C_3H_3 with HCl, is negligibly small under the conditions of the current study, as confirmed in separate experiments. Elevated temperatures were chosen because at lower temperatures the reaction between Cl and propyne (reaction 2b) proceeds through two channels—abstraction and addition; at 500 K and above, abstraction is the only reaction pathway.²¹ The absence of any significant concentration of the addition products was verified by comparing the ion signals of C_3H_3^+ and $\text{C}_3\text{H}_4\text{Cl}^+$ at $m/z = 39$ and $m/z = 75$, respectively.

Separate experiments were performed to evaluate the potential effects of the photodissociation of propyne. Although some production of C_3H_3 was observed, its contribution was minor compared to that of the combination of reactions 2 and 3. The amounts of C_3H_3 produced in the photolysis of propyne were less than 3% (less than 1% at 500 K) of the average concentrations of propargyl radicals used in the experiments to determine the values of k_1 .

Radical precursors and other chemicals used (see below) were obtained from Aldrich (oxalyl chloride, $\geq 99\%$, propyne, 98%, 1-phenyl-1-propyne, 99%, and phenylacetylene, 98%), Matheson (HCl, 99.99%, and ethane, 99%), Lancaster (2,4-hexadiyne, 98%), Fisher Scientific (benzene, $\geq 99\%$), Alfa Aesar (1,5-hexadiyne, 50% solution in pentane), and MG Industries (helium, 99.999%, and nitrogen, 99.999%). Oxalyl chloride, propyne, and ethane were purified by vacuum distillation prior to use. Helium, nitrogen, and other chemicals were used without further purification.

Method of Determination of the Rate Constant. Propargyl radicals were produced by the 248 nm photolysis of the corresponding mixture of precursors diluted in the helium carrier gas. The kinetics of the radical decay was monitored in real time. Rate constant measurements were performed using a technique analogous to that applied by Slagle and co-workers²⁸ to the study of the $\text{CH}_3 + \text{CH}_3$ reaction. The experimental conditions were selected in such a way that the characteristic time of the reaction between Cl and propyne²¹ was at least 27 times shorter (typically, 200 times shorter) than that of the self-reaction of the propargyl radicals. Under these experimental conditions, the self-reaction of C_3H_3 was unperturbed by any side processes, and the only additional sink of the radicals was due to the heterogeneous wall loss, which was taken into account in the analysis. Thus, the experimental kinetic mechanism included reactions



For this kinetic mechanism and initial conditions described above, the corresponding first order differential equations can be solved analytically:

$$S = \frac{S_0 k_w}{(2k' + k_w)e^{k_w t} - 2k'} \quad (I)$$

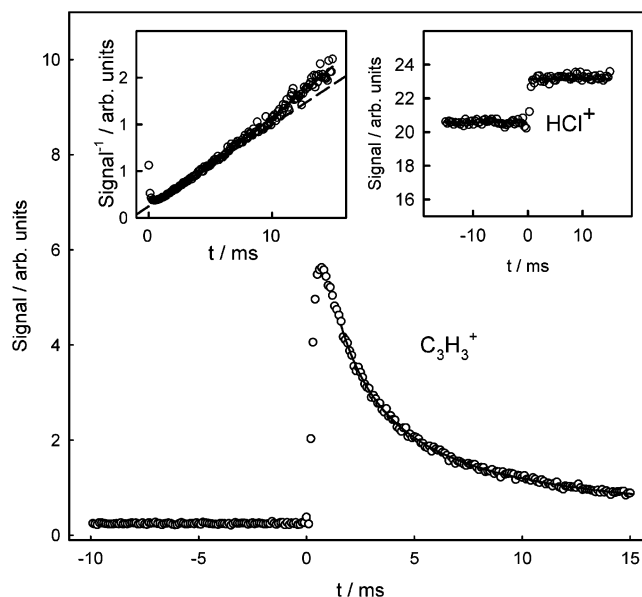


Figure 1. Typical temporal ion signal profiles recorded in an experiment to determine the rate of the $\text{C}_3\text{H}_3 + \text{C}_3\text{H}_3$ reaction. $T = 500$ K, $[\text{He}] = 6.0 \times 10^{16}$, $[\text{C}_3\text{H}_4] = 5.04 \times 10^{15}$, $[(\text{CClO})_2] = 8.31 \times 10^{14}$, and $[\text{C}_3\text{H}_3]_0 = 1.08 \times 10^{13}$ molecules cm^{-3} . The solid curve on the main plot represents a fit of the experimental data with the kinetic mechanism consisting of reactions 1 and 4. The inset on the right shows the increase in the signal of HCl. The inset on the left shows the reciprocal of the ion signal of C_3H_3 as a function of time. The solid curve represents a fit of the experimental data with the kinetic mechanism consisting of reactions 1 and 4. The dashed line represents fitting of the initial part of the signal with a linear dependence (see text).

Here, $k' = k_r[\text{R}]_0$, k_r is the self-reaction rate constant ($r = 1$), $[\text{R}]_0$ is the initial radical concentration, S is the radical ion signal, S_0 is the initial signal amplitude, and k_w is the rate of the wall loss reaction (reaction 4). In each experiment, the values of the initial signal amplitude S_0 , the wall loss rate k_w , and the $k_r[\text{R}]_0$ product were obtained from the fits of the real-time radical decay profile with eq I. Typical signal profiles of HCl and the propargyl radical decay are shown in Figure 1.

Different parts of the radical decay profiles exhibit different sensitivities to the fitting parameters. The initial part of the signal profile is most sensitive to the rate constant of the radical self-reaction whereas the end part is most sensitive to the rate constant of the heterogeneous wall loss of the radicals. These sensitivities are illustrated in the inset in Figure 1, where the reciprocal of the radical signal (with the baseline determined before the photolyzing laser pulse subtracted) is plotted as a function of time. In the absence of any heterogeneous wall loss of radicals (pure second-order decay), the reciprocal signal is directly proportional to time and forms a straight line; the self-reaction rate constant can be obtained from the slope of the line. In the presence of heterogeneous loss, the line is curved, the initial slope is proportional to $(2k' + k_w)$, and the deviation from straight line can serve as a measure of the contribution from the heterogeneous wall loss. As can be seen from the plot in Figure 1, both the slope of the initial part of the reciprocal signal vs time dependence and the deviation from linearity are well characterized, which illustrates that both the $k_r[\text{R}]_0$ and the k_w values can be obtained from the fit of the signal with a high degree of accuracy.

The rate of the heterogeneous loss of radicals (reaction 4) did not depend on the laser intensity or concentrations of radical precursors but was affected by the condition of the walls of the reactor (such as history of the exposure to different reacting

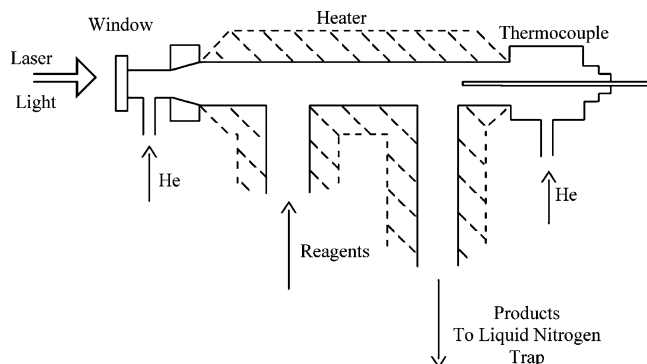


Figure 2. Reactor constructed for the study of the final products of the self-reaction of propargyl radicals.

mixtures). In principle, it was possible to obtain the values of k_4 in separate experiments with low initial radical concentrations selected in such a way as to make the rates of radical self-reactions negligible. However, in the experiments performed to determine the rates of the C_3H_3 self-reaction, a small fraction of the Cl atoms produced in the photolysis of oxalyl chloride decayed on the reactor walls, which could possibly have affected the wall conditions. Thus, it was deemed more appropriate to determine the rates of wall losses of radicals in the same experiments where the rates of radical self-reactions were obtained. Separate experiments with low propargyl concentrations (such that the C_3H_3 self-reaction was negligible) were performed at 500 and 700 K to confirm that the values of k_4 obtained are in general agreement with those derived from the three-parameter fits of radical decays obtained with high C_3H_3 concentrations. The values of k_4 obtained from the fits of the C_3H_3 profiles at 1000 K were, generally, higher, as described and discussed below.

In each experiment, the initial concentration of the C_3H_3 radicals was determined by measuring the production of HCl relative to a calibration standard. This value was obtained directly from the HCl^+ ion profile (Figure 1). In each experiment to determine $k' = k_r[R]_0$, the production of HCl was measured two times (before and after the kinetics of the radical decay was recorded).

For each experimental temperature, the initial radical concentration $[R]_0$ ($R = C_3H_3$) was varied by changing the concentration of oxalyl chloride and/or the laser fluence. The values of the $k_r[R]_0$ product obtained from the data fits were plotted as a function of the initial concentration of radicals obtained from the measurements of the photolytic production of HCl ($[R]_0$). The values of the radical self-reaction rate constant were determined from the slopes of the linear $k_r[R]_0$ vs $[R]_0$ dependences.

Product Analysis. The experimental apparatus employed for the kinetic measurements in the current study permits detection of the products of the propargyl radical self-reaction, but it cannot be used to differentiate between isomers of the same molecular weight and similar ionization potentials. A new experimental apparatus was constructed in order to perform the product analysis of reaction 1 (Figure 2). The objective of the new design was to avoid collection of the products of reactions occurring at low temperatures, which would happen if the original real-time reactor were used. In the real-time reactor, the gas inlets and the reactor window are located outside of the heated zone, and thus it is impossible to avoid the photolysis of the gas mixture in the cold zone. This photolysis of the cold part of the gas mixture has no consequence for the kinetic measurements because, in these measurements, only the heated

part of the gas mixture is analyzed during short time following the laser pulse.

The dimensions of the tubular heated quartz reactor (i.d. 1.0 cm) were selected such that experiments could be performed at a high laser firing frequency. The reacting mixture is preheated in a short inlet before entering the reactor zone where it is photolyzed. The mixture in the photolysis zone is completely replaced between the laser pulses. Small flows of helium, which are also preheated, are introduced through the "window" inlet and through the "thermocouple" inlet (opposite to the reactor window). These flows (a) create buffer zones next to the reactor window and around the thermocouple where no reaction takes place, (b) eliminate possible problems due to photolysis of the reactants on the rear wall of the reactor, opposite the laser source, and (c) eliminate the stagnation zones that otherwise would be created next to the reactor window and around the thermocouple inlet. The products of the reaction were collected in a liquid nitrogen trap at the exit of the heated reactor end perpendicular to the zone of photolysis. The length of the heated product outlet was selected such that more than 99% of the propargyl radicals created during photolysis would decay due to recombination and heterogeneous loss before the reacting mixture reaches a cold zone. The residence times were ~ 120 ms in the heated zone of the reactor and ~ 100 ms in the room temperature zone between the reactor and the liquid nitrogen trap.

Species accumulated in the trap were transferred to a gas sampling vial and diluted with helium to atmospheric pressure. The samples were then analyzed by a Hewlett-Packard GC/MS (5890 series II/5889B) equipped with an Agilent GasPro column (i.d. 0.32 mm, 30 m length). The experiments were conducted at a laser frequency of 15 Hz. The products of reaction 1 were analyzed at 500, 700, 900, 1000, and 1100 K. Experiments were conducted at a bath gas density of 6.0×10^{16} molecules cm^{-3} , oxalyl chloride concentrations of $(1.8-2.1) \times 10^{15}$ molecules cm^{-3} , and propyne concentrations of $(4.7-5.4) \times 10^{15}$ molecules cm^{-3} .

Knowledge of the reaction products mass spectra and retention times is necessary for the GC/MS analysis. C_6H_6 isomers along with the phenyl radical and H atoms are expected to be the major products of the $C_3H_3 + C_3H_3$ reaction according to the results of Alkemade and Homann,⁴ Fahr and Nayak,⁵ and those of the theoretical studies.^{7,8,16,17} Only three of the possible C_6H_6 isomers were available commercially: benzene (Fisher Scientific), 2,4-hexadiyne (Lancaster), and 1,5-hexadiyne (Alfa Aesar); samples of these species were purchased and used in the analysis. Two more isomers, 1,2-dimethylenecyclobutene and fulvene, were synthesized by thermal isomerization of 1,5-hexadiyne.⁶ In the synthesis, the conditions of the study of Stein et al.⁶ were reproduced. The same reactor as that used for the product analysis (but filled with glass beads) was used. The flow velocity was selected to achieve a reactor residence time of the mixture of the 1,5-hexadiyne vapor in nitrogen equal to 30 s. The reactor was heated to 700 and 850 K at atmospheric pressure; laser photolysis was not used in this series of experiments. 1,2-Dimethylenecyclobutene is expected to be the major product at 700 K, and a $\sim 2:1$ mixture of fulvene and benzene is expected at 850 K. The products were collected in a liquid nitrogen trap, transferred to a sampling vial, diluted with helium to atmospheric pressure, and analyzed by GC/MS. By comparing the results of the GC/MS analysis of the products of thermal isomerization obtained in the current study with the results of Stein et al.⁶ (who used synthesized samples of C_6H_6 isomers to identify the observed products), it was possible to

obtain the retention times and the mass spectra of fulvene and 1,2-dimethylenecyclobutene as well as an approximate sensitivity of the mass spectrometer toward fulvene (relative to benzene). Thermal decomposition of oxalyl chloride becomes efficient at temperatures above 1000 K; therefore, it was used as a source of Cl atoms at 1100 K in the experiments on the analysis of the products of the $C_3H_3 + C_3H_3$ reaction instead of laser photolysis.

III. Experimental Results

$C_3H_3 + C_3H_3$ Reaction Rate. The values of the rate constant of reaction 1 were obtained at 500, 700, and 1000 K and bath gas densities (mostly helium, balance radical precursors) of 3×10^{16} and 6×10^{16} molecules cm^{-3} . Experimental parameters such as the photolyzing laser intensity and the concentrations of oxalyl chloride and propyne were varied for individual experiments. For each temperature, the values of the $k_t[R]_0$ product obtained under different experimental conditions (including different bath gas densities) are shown on the same $k_t[R]_0$ vs $[R]_0$ plots in Figures 3–5. The rate constant of the propargyl radical self-reaction does not demonstrate any dependence (within the experimental uncertainties) on the parameters varied; no pressure dependence of k_1 can be observed within the experimental uncertainties. The conditions and the results of individual experiments are presented in Table 1. The values of k_1 determined from the slopes of the $k_t[R]_0$ vs $[R]_0$ dependences are also given in Table 1 for the three experimental temperatures. The overall temperature dependence of the rate constant obtained is shown in Figure 6.

Relatively high values of the heterogeneous wall loss rate (Table 1) and larger $C_3H_3^+$ signal background were observed in the experiments performed at 1000 K. This phenomenon was attributed to thermal decomposition of oxalyl chloride, which created an additional source of Cl atoms (and, consequently, propargyl radicals) both before and after the laser pulse. Under these conditions, the kinetics of the propargyl radical decay after the laser pulse corresponded to relaxation to the steady-state concentration determined by the balance between the production caused by the thermal decomposition of $(CClO)_2$ and destruction due to recombination and wall loss. Typical steady-state concentrations of C_3H_3 due to the $(CClO)_2$ decomposition were less than 7% of the initial concentration of propargyl radicals created photolytically via reactions 2 and 3. The presence of the additional thermal source of propargyl radicals alone does not affect the determined values of the rate constant of reaction 1, as discussed below (see Discussion). However, secondary reactions of the products of reaction 1 could have affected the kinetics observed at 1000 K. Possible effects of the secondary chemistry on the rate constant of the propargyl radical self-reaction are discussed in section IV (Discussion).

Products. C_6H_6 isomers, phenyl radical, and hydrogen atom are expected as the products of the $C_3H_3 + C_3H_3$ reaction.^{4–8,16} An example of a signal of $C_6H_6^+$ detected in real-time experiments is shown together with the corresponding profile of the $C_3H_3^+$ decay in Figure 7. No C_6H_5 (phenyl radical) could be detected; under the experimental conditions employed in the current study, phenyl radicals are expected to quickly react (reaction rate $> 10^3 s^{-1}$ at $T > 800 K$)²⁹ with the excess of propyne present in the reactor. The results of the GC/MS analysis of the final product mixture collected in the liquid nitrogen trap from the experiments performed at 500, 700, 900, 1000, and 1100 K are presented in Table 2, and the values of relative fractions of different C_6H_6 isomers (based on the total GC/MS ion count) are plotted as functions of temperature in

TABLE 1: Conditions and Results of Experiments To Determine k_1

[M] ^a	I ^b	[C ₃ H ₃] ^c	[(CClO) ₂] ^d	[HCl] ^e	[C ₃ H ₃] ^f	$k_t[R]_0$ ^g	k_w ^h
Experiments at 500 K							
6.0	117	4.91	4.86	10.25	0.71 ± 0.04	235 ± 17	22 ± 3
6.0	108	4.91	7.16	10.30	0.97 ± 0.03	337 ± 23	23 ± 4
6.0	121	5.14	7.53	5.81	1.15 ± 0.02	363 ± 26	22 ± 4
6.0	133	4.51	3.89	8.66	0.65 ± 0.01	203 ± 6	20 ± 2
6.0	103	5.04	8.31	8.42	1.08 ± 0.05	367 ± 19	19 ± 3
6.0	94	4.14	8.86	8.36	1.05 ± 0.03	348 ± 18	19 ± 3
6.0	82	4.58	11.40	8.26	1.18 ± 0.17	364 ± 22	21 ± 3
6.0	62	4.17	9.48	8.21	0.75 ± 0.01	288 ± 20	23 ± 4
6.0	92	1.00	6.72	7.92	0.78 ± 0.08	246 ± 9	58 ± 2
6.0	110	0.99	8.41	8.44	1.16 ± 0.12	362 ± 17	72 ± 2
3.0	107	3.82	4.63	10.85	0.47 ± 0.05	180 ± 15	27 ± 5
3.0	133	4.68	7.15	8.44	0.83 ± 0.02	344 ± 36	9 ± 6
3.0	117	4.30	6.26	5.39	0.59 ± 0.05	197 ± 13	17 ± 4
3.0	133	4.44	9.83	6.19	1.06 ± 0.14	309 ± 21	27 ± 4
$k_1(500 K) = (3.30 \pm 0.35) \times 10^{-11} cm^3 molecule^{-1} s^{-1}$							
Experiments at 700 K							
6.0	133	5.51	8.30	10.10	0.93 ± 0.04	253 ± 9	2 ± 2
6.0	107	4.53	8.76	10.10	0.71 ± 0.01	226 ± 12	0 ± 4
6.0	133	4.66	8.46	10.60	0.61 ± 0.02	182 ± 12	5 ± 5
6.0	133	5.06	7.92	9.77	0.93 ± 0.09	274 ± 12	4 ± 3
6.0	113	4.61	6.62	10.80	0.70 ± 0.17	150 ± 15	19 ± 6
6.0	123	4.65	8.09	9.37	0.89 ± 0.11	241 ± 13	5 ± 4
6.0	51	4.80	10.80	11.50	0.43 ± 0.06	161 ± 8	-6 ± 4
6.0	127	4.80	10.80	10.80	1.15 ± 0.14	307 ± 27	4 ± 5
6.0	120	5.42	13.40	10.60	1.30 ± 0.10	337 ± 16	4 ± 3
$k_1(700 K) = (2.74 \pm 0.43) \times 10^{-11} cm^3 molecule^{-1} s^{-1}$							
Experiments at 1000 K							
6.0	120	4.58	41.70	5.60	3.17 ± 0.16	410 ± 13	77 ± 2
6.0	48	4.58	41.70	5.78	0.73 ± 0.10	98 ± 6	89 ± 4
6.0	47	5.08	38.30	5.04	0.80 ± 0.08	100 ± 10	102 ± 5
6.0	26	5.08	38.30	5.48	0.77 ± 0.13	110 ± 11	94 ± 5
6.0	117	4.00	23.90	5.58	2.01 ± 0.51	252 ± 10	14 ± 3
6.0	117	4.00	23.90	4.83	0.99 ± 0.01	122 ± 7	87 ± 4
6.0	113	2.27	24.20	5.54	1.01 ± 0.01	118 ± 9	85 ± 4
6.0	113	3.76	23.60	5.02	1.06 ± 0.01	131 ± 5	89 ± 2
6.0	70	3.67	26.30	4.99	2.39 ± 0.20	306 ± 19	71 ± 4
6.0	64	3.90	29.00	24.00	2.31 ± 0.13	277 ± 22	82 ± 5
6.0	107	3.90	22.20	26.9	3.48 ± 0.33	382 ± 23	74 ± 4
6.0	117	4.06	16.70	26.8	2.92 ± 0.23	331 ± 21	78 ± 4
6.0	117	4.06	7.15	25.2	1.25 ± 0.09	156 ± 13	38 ± 6
3.0	117	2.42	17.00	25.4	1.66 ± 0.02	141 ± 14	64 ± 6
3.0	117	2.42	20.90	24.8	1.85 ± 0.02	179 ± 14	55 ± 5
3.0	117	4.62	32.90	24.8	2.65 ± 0.61	362 ± 25	51 ± 5
3.0	47	4.62	32.90	25.8	1.01 ± 0.06	156 ± 13	38 ± 6
3.0	117	3.93	28.20	26.0	1.90 ± 0.08	206 ± 11	61 ± 4
3.0	117	4.24	30.40	25.6	2.30 ± 0.07	296 ± 18	60 ± 4
3.0	70	4.24	30.40	24.3	1.14 ± 0.07	105 ± 10	78 ± 2
$k_1(1000 K) = (1.20 \pm 0.14) \times 10^{-11} cm^3 molecule^{-1} s^{-1}$							

^a Concentration of the bath gas (mostly helium, balance radical precursors) in units of 10^{16} atoms cm^{-3} . ^b Estimated laser fluence in units of $mJ pulse^{-1} cm^{-2}$. ^c In units of 10^{15} molecules cm^{-3} . ^d In units of 10^{14} molecules cm^{-3} . ^e Concentration of the internal standard (in units of 10^{13} molecules cm^{-3}). ^f Nascent concentration of propargyl radicals in units of 10^{13} molecules cm^{-3} determined from production of HCl. Uncertainties are 2σ (statistical) + systematic. ^g Obtained from the fits of the kinetics of the C_3H_3 decay with eq 1. Uncertainties are 1σ (statistical) from the curve fitting. ^h Rate constant of the heterogeneous wall loss obtained from the fits of the kinetics of the C_3H_3 decay with eq 1. Uncertainties are 1σ (statistical) from the curve fitting. ⁱ Uncertainties are 2σ (statistical) + systematic.

Figure 8. Benzene, fulvene, and 1,5-hexadiyne were identified by their retention times and ion fragmentation patterns. 2,4-Hexadiyne and 1,2-dimethylenecyclobutene were not detected among the products of the propargyl radical self-reaction. Two unknown species (identified below as unknown 1 and unknown 2) with ion fragmentation patterns characteristic of species with the elemental composition of C_6H_6 were detected but could not

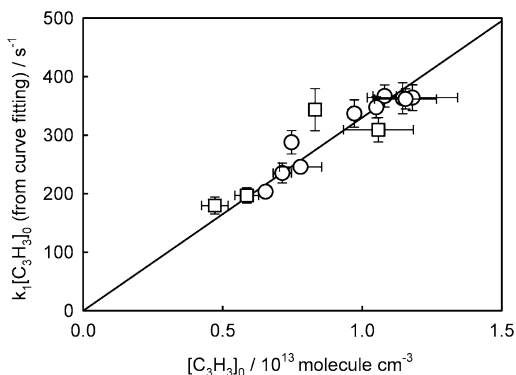


Figure 3. $k_1[\text{C}_3\text{H}_3]_0$ vs $[\text{C}_3\text{H}_3]_0$ dependence obtained in the study of reaction 1 at 500 K: circles, bath gas density of 6.0×10^{16} molecules cm^{-3} ; squares, bath gas density of 3.0×10^{16} molecules cm^{-3} .

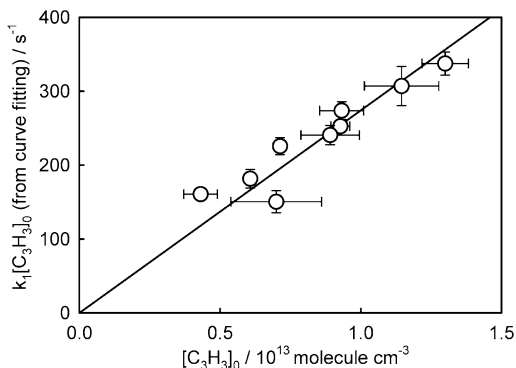


Figure 4. $k_1[\text{C}_3\text{H}_3]_0$ vs $[\text{C}_3\text{H}_3]_0$ dependence obtained in the study of reaction 1 at 700 K. The bath gas density is 6.0×10^{16} molecules cm^{-3} .

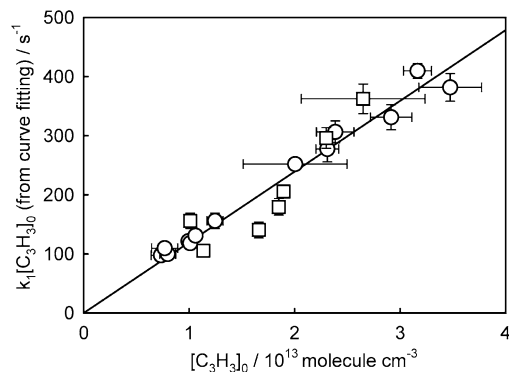


Figure 5. $k_1[\text{C}_3\text{H}_3]_0$ vs $[\text{C}_3\text{H}_3]_0$ dependence obtained in the study of reaction 1 at 1000 K: circles, bath gas density of 6.0×10^{16} molecules cm^{-3} ; squares, bath gas density of 3.0×10^{16} molecules cm^{-3} .

be identified due to the lack of standard compounds. The sensitivity (relative to benzene) of the mass spectrometer toward 1,5-hexadiyne (0.8) was evaluated by analyzing a prepared mixture of 1,5-hexadiyne and benzene; the relative sensitivity toward fulvene (~ 1) was estimated on the basis of the analysis of the products of the thermal isomerization experiments (see section II).

Although 1,2-dimethylenecyclobutene was not detected among the products, the results of the experiments cannot completely rule out its formation in small amounts. The chromatographic column used in the current study could not completely resolve 1,2-dimethylenecyclobutene and benzene: when the mixture of products obtained in the experiments on the thermal isomerization of 1,5-hexadiyne was analyzed, the peaks of these two species partially overlapped. 1,2-Dimethylenecyclobutene has a somewhat shorter retention time than benzene and a different MS spectrum. Thus, different sides of the combined 1,2-

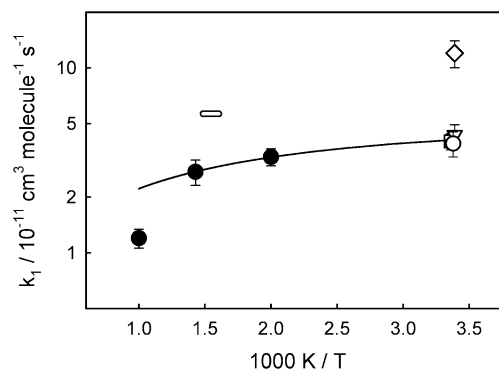


Figure 6. Temperature dependence of the experimentally obtained values of k_1 (filled circles). Diamond, inverted triangle, square, open circle, and short white line represent the values of k_1 reported in refs 10, 11, 5, 13 and 4, respectively. The solid line represents the fit of eq II.

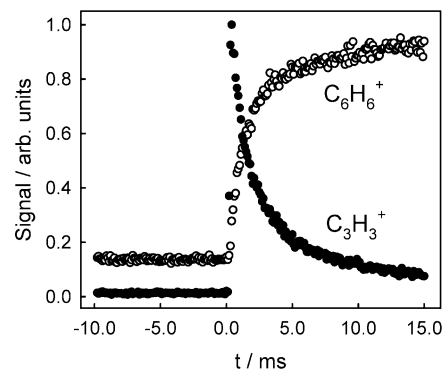


Figure 7. Typical temporal ion signal profiles of C_3H_3 and C_6H_6 recorded in an experiment to study the products of the $\text{C}_3\text{H}_3 + \text{C}_3\text{H}_3$ reaction. $T = 1000$ K, bath gas density is 6.0×10^{16} , $[\text{C}_3\text{H}_4] = 4.62 \times 10^{15}$, $[(\text{CClO})_2] = 1.68 \times 10^{15}$, and $[\text{C}_3\text{H}_3]_0 = 1.12 \times 10^{13}$ molecules cm^{-3} .

TABLE 2: Relative Ion Counts of Different C_6H_6 Isomers in the Propargyl Radical Self-Reaction As Determined by the GC/MS Analysis of the Final Products

	T/K				
	500	700	900	1000	1100
benzene	26	30	82	85	87
1,5-hexadiyne	31	19	4	4	1
fulvene	0	0	9	6	7
unknown 1	43	50	2	1	1
unknown 2	0	0	2	4	4

dimethylenecyclobutene/benzene peak exhibited different MS spectra. On one side of the peak, an ion fragment pattern characteristic of benzene was obtained. The MS spectrum obtained on the other side was assigned to 1,2-dimethylenecyclobutene. On the chromatograms of the products obtained in the experiments on the C_3H_3 self-reaction, peaks of benzene (identified by both the retention time and the MS spectrum) did not exhibit any variations in the MS spectrum along the scale of retention times within the same peak. This indicates that 1,2-dimethylenecyclobutene is not a major product under any conditions used. However, the presence of minor amounts of 1,2-dimethylenecyclobutene obscured on the chromatogram by larger peaks of benzene cannot be completely ruled out.

At 500 and 700 K unknown 1 was detected as the major product (43% and 50%) of the $\text{C}_3\text{H}_3 + \text{C}_3\text{H}_3$ reaction; 1,5-hexadiyne and benzene respectively were 31% and 26% of the total ion count at 500 K and 19% and 30% at 700 K. At the temperatures of 900 K and above benzene becomes the major product of the $\text{C}_3\text{H}_3 + \text{C}_3\text{H}_3$ reaction (more than 80%) with

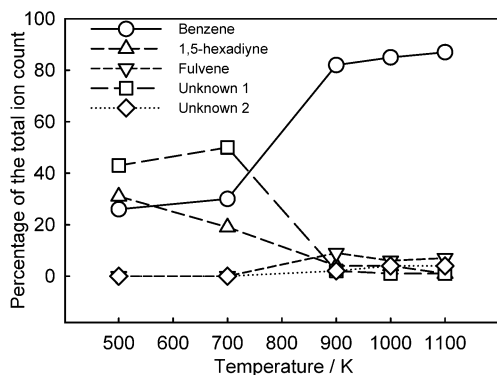


Figure 8. Temperature dependence of the C_6H_6 product fractions of the $C_3H_3 + C_3H_3$ reaction based on the total GC/MS ion count obtained in the final product analysis (data of Table 2).

the fractions of unknown 1 and 1,5-hexadiyne dropping to 1–4%. Fulvene and unknown 2 are detected only at temperatures of 900 K and above. It should be noted that black deposits in the reactor were observed at temperatures of 700 K and above, indicating possible absorption of some of the products on the reactor walls.

Observation of minor amounts of 1,5-hexadiyne and unknown 1 at high temperatures (900 K and above) can potentially be explained by incomplete recombination of the propargyl radicals in the heated zone of the reactor. The length of the reactor and the conditions were selected to provide more than 99% of the radical decay in the heated zone (120 ms residence time). However, calculation of these conditions was based on expected values of radical concentrations, the value of k_1 obtained at 1000 K in the real-time experiments, and an expected propargyl wall loss rate of 20 s^{-1} . If, for example, the actual wall loss of propargyl were close to zero, the conditions in the reactor would correspond to $\sim 98\%$ recombination of C_3H_3 in the heated zone. This can explain the appearance of the small quantities of low-temperature products among those of the high-temperature experiments.

In the GC/MS experiments, C_8H_6 and C_9H_8 were detected among the final products at 1000 and 1100 K. The real-time experiments at 1000 K also demonstrated formation of these species. C_8H_6 and C_9H_8 were not observed at lower temperatures in the GC/MS analysis but were detected in minor amounts in the real-time experiments at 700 K. (The ratio of the signal of C_9H_8 to that of HCl was more than 6 times lower at 700 K compared to that obtained at 1000 K.) The GC/MS analysis suggests that C_8H_6 and C_9H_8 are phenylacetylene and phenyl-1-propyne. The presence of these species can be attributed to formation of C_6H_5 in reaction 1 at elevated temperatures with a subsequent fast reaction of the phenyl radical with propyne²⁹ (see section IV).

IV. Discussion

This work presents the first direct real-time experimental determination of the rate constant and determination of the product distribution of the $C_3H_3 + C_3H_3$ reaction (k_1) as functions of temperature.¹⁸ In this section, first, the values of the rate constant of reaction 1 obtained in the current study are compared with those published previously. Next, the results of the product study are discussed and compared with the results of the earlier experimental and theoretical investigations. Finally, possible effects of the thermal decomposition of oxalyl chloride on the kinetics of propargyl radicals observed at 1000 K and those of secondary reactions are discussed.

Temperature Dependence of the Rate Constant. The values of the rate constant obtained in the current work are shown together with those reported in earlier studies (see section I, Introduction) in Figure 6. As can be seen from the plot, the values of the rate constants of the propargyl radical self-reaction obtained at 500 K ($(3.30 \pm 0.35) \times 10^{-11}\text{ cm}^3\text{ molecule}^{-1}\text{ s}^{-1}$) and at 700 K ($(2.74 \pm 0.43) \times 10^{-11}\text{ cm}^3\text{ molecule}^{-1}\text{ s}^{-1}$) correlate well with the room temperature values of Fahr and Nayak ($(4.0 \pm 0.4) \times 10^{-11}\text{ cm}^3\text{ molecule}^{-1}\text{ s}^{-1}$),⁵ Atkinson and Hudgens ($(4.3 \pm 0.6) \times 10^{-11}\text{ cm}^3\text{ molecule}^{-1}\text{ s}^{-1}$),¹¹ and DeSain and Taatjes ($(3.9 \pm 0.6) \times 10^{-11}\text{ cm}^3\text{ molecule}^{-1}\text{ s}^{-1}$).¹³ The results of the current study, together with those of refs 5, 11, and 13, can be represented by the following modified Arrhenius expression over the 295–700 K temperature interval:

$$k_1^\infty = 4.49 \times 10^{-9} T^{-0.75} \exp(-128\text{ K}/T) \text{ cm}^3 \text{ molecule}^{-1} \text{ s}^{-1} \quad (\text{II})$$

The temperature dependence of eq II is shown in Figure 6 by a solid line.

The values of k_1^∞ demonstrate a moderate decrease with temperature, as can be expected for a barrierless radical–radical reaction. On the other hand, the theoretical studies of Miller and Klippenstein^{16,17} predict a slightly positive temperature dependence. This predicted increase of k_1^∞ with temperature is caused by the particular choice of the functional representation of the part of the potential energy surface responsible for bond breaking, and, as noted by the authors of ref 16, may or may not be correct. The results of Giri et al.¹⁴ seem to indicate a slight increase of the rate constant of reaction 1 with temperature over the 373–520 K range. The rate constant value of ref 14 obtained at 500 K is in agreement with that of the current work. No suggestions can be offered at this time for the origins of the different temperature trends in k_1^∞ derived, on one hand, from the results of the current study and those of refs 5, 11, and 13, and, on the other hand, from the results of Giri et al.¹⁴

The room temperature value of Morter et al.¹⁰ ($(1.2 \pm 0.2) \times 10^{-10}\text{ cm}^3\text{ molecule}^{-1}\text{ s}^{-1}$) is significantly larger. Atkinson and Hudgens¹¹ analyzed the experiments of Morter et al. and suggested that the value of k_1 reported in ref 10 may be overestimated due to the effects of side reactions of secondary photoproducts or to the presence of additional sinks of propargyl radicals caused by trace amounts of toluene, which was used as a solvent for the radical precursor in ref 10.

Alkemade and Homann⁴ were the first to report the value of the rate constant of reaction 1 at elevated temperatures. These authors, however, did not obtain a temperature dependence of the rate constant; the value of $k_1 = 5.6 \times 10^{-11}\text{ cm}^3\text{ molecule}^{-1}\text{ s}^{-1}$ (with no experimental uncertainty) was reported at the temperatures of 623–673 K. This value is larger than those obtained in the current study; unfortunately, discussion of the differences is hampered by the unknown uncertainties of ref 4. The high-temperature estimate of the k_1 value obtained in the shock tube experiments of Scherer et al.¹² ($k_1 \approx (7.5\text{--}15) \times 10^{-12}\text{ cm}^3\text{ molecule}^{-1}\text{ s}^{-1}$ at $T = 1100\text{--}2100\text{ K}$ and pressures of 1.5–2.2 bar) corresponds to conditions that significantly differ from those of the current study (higher temperatures and pressures). Direct comparison of the results would not be meaningful; master equation modeling of the effects of pressure and temperature on the kinetics and products of reaction 1 is needed for an analysis of agreement and/or differences.

The low value of the rate constant at 1000 K obtained in the current work ($(1.20 \pm 0.14) \times 10^{-11}\text{ cm}^3\text{ molecule}^{-1}\text{ s}^{-1}$) is likely to be caused by the falloff effects, as predicted in the

master equation study of Miller and Klippenstein.¹⁶ Also, according to ref 16, reaction 1 should be in the high-pressure limit at 500 and 700 K at the experimental pressures employed in the current study. It should be noted that the value of k_1 obtained in the experiments performed at 1000 K should be treated with caution as secondary reactions could have affected the kinetics of C_3H_3 at this temperature. Potential effects of these secondary reactions are discussed below.

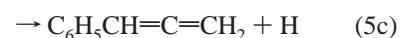
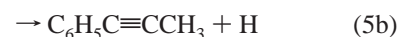
Product Analysis. Earlier experimental studies of the products of the self-reaction of propargyl radicals include those of Alkemade and Homann⁴ (performed at 623–673 K) and Fahr and Nayak⁵ (room temperature). A theoretical study of Miller and Klippenstein¹⁶ used the potential energy surface of Miller and Melius⁷ and Melius et al.⁸ and master equation calculations to evaluate temperature and pressure dependences of the kinetics and products of reaction 1. The authors of these studies^{7,8,16} distinguish three possible initial pathways of propargyl recombination: “head to head”, “tail to tail”, and “head to tail” (using terminology from refs 7 and 8 where the “head” is the CH_2 end and “tail” is the CH end of the propargyl radical). Following the initial recombination step, products of the $C_3H_3 + C_3H_3$ reaction can stabilize by collisions with the bath gas or undergo isomerization into various C_6H_6 isomers.

The “head-to-head” and “tail-to-tail” recombination channels result in the initial formation of 1,5-hexadiyne and 1,2,4,5-hexatetraene, respectively. These intermediates can be expected^{7,8,16} to easily isomerize into each other; 1,2,4,5-hexatetraene can also undergo a reversible isomerization into 1,2-dimethylenecyclobutene. The “head-to-tail” channel leads to the initial formation of 1,2-hexadiene-5-yne, which can isomerize (reversibly) to 2-ethynyl-1,3-butadiene. Both 1,2,4,5-hexatetraene and 1,2-hexadiene-5-yne can isomerize to fulvene, which can be followed by fulvene-to-benzene isomerization and decomposition of benzene into phenyl radical and H atom. Thus, reactive pathways to fulvene, benzene, and phenyl radical are open to all three initial recombination channels.

Fahr and Nayak⁵ observed 1,5-hexadiyne (60% relative yield), 1,2-hexadiene-5-yne (25%), and an unknown C_6H_6 isomer (15%) as products of reaction 1 at room temperature. Alkemade and Homann⁴ reported formation of benzene (19–30%), 1,5-hexadiyne (2–11%), 1,2-hexadiene-5-yne (30–46%), 1,2,4,5-hexatetraene (7–19%), and 1,3-hexadiene-5-yne (15–19%) among the products of the $C_3H_3 + C_3H_3$ reaction at 623–673 K and the pressures of 2–4 Torr. The authors of ref 4 used the reaction of propargyl halides with sodium vapor to generate C_3H_3 radicals and gas chromatography/mass spectrometry to study the final products of reaction 1. The temperature and pressure ranges employed in the experiments of Alkemade and Homann overlap with the conditions used in the current study, allowing a direct comparison of the results. In the current study, between the temperatures of 500 and 700 K unknown 1 was detected as the major C_6H_6 product of the propargyl radical self-reaction (43–50% of the ion count); comparison with the results of ref 4 suggests that it can be 1,2-hexadiene-5-yne, the product of the head-to-tail recombination. Benzene was detected in similar amounts in the current study (26–30%) and in ref 4 (19–30%). The yield of 1,5-hexadiyne reported in ref 4 (2–11%) is reasonably close to that obtained in the current study at 700 K (19%). On the other hand, Alkemade and Homann report more products than were detected in the current work under similar conditions, which undermines the suggestion of equality between unknown 1 and 1,2-hexadiene-5-yne. As the temperature increases, the fractions of unknown 1 and 1,5-hexadiyne drop to 1–4% and benzene becomes the dominant product. This

indicates that unknown 1 is likely to be one of the “early” intermediates on the reaction PES; in addition to 1,2-hexadiene-5-yne suggested above, 1,2,4,5-hexatetraene or 2-ethynyl-1,3-butadiene can be proposed as candidates. Ion fragmentation patterns observed in the GC/MS analysis of the C_6H_6 isomers obtained from commercial sources, in thermal isomerization experiments, and in the product study of reaction 1 are presented in the Supporting Information. Thus, future experimental studies may help identify the chemical structures of the unknown 1 and the unknown 2 species.

The presence of phenylacetylene and phenyl-1-propyne among the products detected in the current study at elevated temperatures can be attributed to the formation of phenyl radical in reaction 1 and its subsequent reaction with propyne. Reaction of phenyl with propyne can proceed via several channels:²⁹



There are no experimental data available on this reaction. A recent theoretical study by Vereecken et al.²⁹ predicts comparable yields of all these channels, complicating the analysis of the products of the reaction system used in the current study.

In principle, it is possible to estimate the phenyl-to- C_6H_6 branching ratio in reaction by measuring the yields of C_8H_6 and C_6H_6 (either in final product analysis or in real-time experiments) and using theoretical values of the channel branching fractions in reaction 5. However, such an estimate would heavily rely on the accuracy of the theoretical values, the uncertainties of which are unknown. Therefore, no attempts to determine the relative yields of phenyl radical and benzene were performed in the current study. Experimental data on reaction 5 are needed for such an analysis to be meaningful.

It can be noted that the channel of reaction 1 producing phenyl radical becomes important only at high temperatures. C_8H_6 and C_9H_8 were detected among the final products only at 1000 K and above. Although weak signals of these species were detected in real-time experiments at 700 K, their amplitudes were significantly less than at 1000 K.

It is instructive to compare the results of the current study with the theoretical predictions of Miller and Klippenstein.¹⁶ The general trends in the product distribution as a function of temperature are in agreement. At low temperatures, products of addition and, possibly, initial steps of isomerization are favored. At high temperatures, benzene becomes the dominant product; evidence for the formation of phenyl radicals is also observed. Fulvene is detected among the products. These observations are in agreement with the theoretical model.¹⁶ At the same time, there are quantitative differences in the values of product yields between the predictions and the observations. The main disagreement between the experimental results of the current study and the theoretical predictions is that theory predicts significantly more fulvene than experimentally detected, even at low temperatures, and less benzene than found experimentally. These differences can be attributed to the potential energy surface (PES) used in the theoretical calculations. On the PES used in ref 16, the only pathway leading to benzene passes through fulvene. In a recent theoretical study by the same authors,¹⁷ the PES of reaction 1 was extensively explored by quantum chemical methods. As a result, new pathways and intermediates have been found, including a

pathway leading to benzene without passing through fulvene. It can be expected that theoretical modeling of reaction 1 based on the new PES information and calibrated against the experimental data on the rates and products of reaction obtained in this and other^{4,5,11,13–15} studies will result in agreement with experiment and, thus, in the creation of a comprehensive and predictive model of the self-reaction of propargyl radicals.

In interpreting the results of this and other product studies, one should keep in mind that, under certain conditions, the primary products of reaction 1 can undergo further thermal isomerization. It is important to distinguish the primary products and those of their further transformations. In particular, isomerization of 1,5-hexadiyne and 1,2-dimethylenecyclobutene is known to occur at moderate and high temperatures;⁶ isomerization of fulvene to benzene requires higher temperatures.³⁰ Another potential low-temperature product of reaction 1, 1,2,4,5-hexatetraene, has a low barrier to isomerization (22 kcal mol⁻¹ on the PES of refs 7 and 8 and 30 kcal mol⁻¹ on the PES of ref 17). The recent study of Miller and Klippenstein¹⁷ predicts the rate of thermal isomerization of 1,2,4,5-hexatetraene to 1,2-dimethylenecyclobutene at 50 Torr to be ~0.25 s⁻¹ at 500 K and ~1000 s⁻¹ at 700 K. The residence time of the reactive gas mixture in our experiments on the final products of reaction 1 was ~120 ms, which would correspond to negligible thermal isomerization at 500 K and complete isomerization at 700 K. Experiments conducted in equipment with longer residence times can result in significantly different final products. This discussion serves not to describe the actual processes occurring in the experiments of the current study (as the identity of the unknown 1 product cannot be specified at this time) but to emphasize the importance of accounting for exact experimental conditions, including the residence time, in interpreting the results of different experimental investigations. Another factor that, potentially, can limit the usefulness of experimental information for the development of theoretical models is the effect of heterogeneous chemistry. Radicals decaying on the walls (in the current study, a small fraction), generally, react in unknown ways; products of these wall reactions can remain adsorbed or become released into the gas phase. Moreover, heavy polyatomic products can adsorb on the walls and thus avoid detection. As was mentioned above, in the current study, black wall deposits were detected at the temperatures of 700 K and above, indicating that a fraction of the products avoided detection. It is likely that heavier compounds such as those resulting from further reactions of phenyl radical (C₈H₆ and C₉H₈) were affected. Because of the unknown identity of some of the products, the carbon balance could not be verified in the current study. Another potential effect complicating analysis can be the heterogeneous thermal isomerization of products. Generally, heterogeneous effects cannot be completely avoided in final product studies performed at low pressures or at high pressures with long residence times.

Kinetics of Reaction 1 at 1000 K: Effects of Thermal Decomposition of Oxalyl Chloride and Secondary Chemistry. Effects of thermal decomposition of oxalyl chloride were observed in the current study at the highest temperature used in the real-time kinetic experiments, 1000 K. The products of thermal decomposition are expected to be the same as those of reaction 2, i.e., Cl and CO. The chlorine atoms react with the excess of propyne present in the reactor (reaction 3) and thus generate propargyl radicals. This “thermal” source starts producing C₃H₃ as the gas mixture enters the heated zone of the reactor. The radicals thus generated decay due to self-reaction and wall loss. A steady-state concentration determined by the balance

of production and decay is thus established; it is present in the reactor prior to the photolyzing laser pulse. The laser photolysis of (CClO)₂ followed by reaction 3 creates an additional amount of propargyl radicals. Thus, the kinetics of subsequent decay of C₃H₃ is that of relaxation to the steady-state concentration.

The kinetics of C₃H₃ in such a system with a thermal source can be described by the following equation:

$$\frac{dx}{dt} = -2k_1x^2 - k_4x + \alpha \quad (\text{III})$$

Here, x is the C₃H₃ concentration, k_1 and k_4 are the rate constants of reaction 1 and the heterogeneous wall loss of C₃H₃, respectively, and α is the rate of production of C₃H₃ due to the thermal decomposition of oxalyl chloride.

Substituting $x = y + \beta$ and choosing the value of β to satisfy the requirement $\alpha = k_4\beta + 2k_1\beta^2$, we obtain

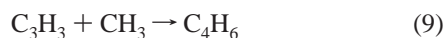
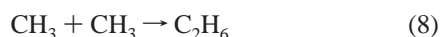
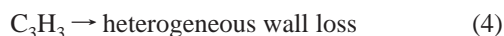
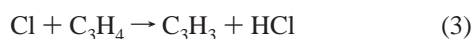
$$\frac{dy}{dt} = -2k_1y^2 - \gamma y \quad (\text{IV})$$

where $\gamma = k_4 + 4k_1\beta$ is a constant. Equation IV has the form equivalent to that of the differential equation describing the kinetics of the self-reaction (with the rate constant k_1) and the first-order loss (with the rate constant γ) of species with concentration equal to y . Analysis of eqs III and IV demonstrates that, prior to the laser pulse, the steady-state concentration of C₃H₃ in the presence of the thermal source is equal to β (thus $y = 0$) and, in the limit of $t \rightarrow \infty$, also $x = \beta$ and $y = 0$. In the experiments to determine the rate constant of reaction 1, the signal of propargyl radicals measured before the laser pulse is subtracted from that observed after the laser pulse to obtain the $S(t)$ dependence; the resultant $S(t)$ kinetic curves are fitted with eq I. Thus, S can be identified with y ; fitting of the $S(t)$ dependences obtained in the presence of the thermal source with eq I should produce the correct values of k_1 and “effective” values of heterogeneous wall loss rate (γ) that are larger than the real values of k_4 , as observed in the experiments. The above derivation serves to demonstrate that the presence of a thermal source of propargyl radicals does not result in errors in the determination of the rate constant.

The mathematical derivation shown above was made under the assumption that the concentration of C₃H₃ due to thermal decomposition of oxalyl chloride attains steady state by the time the reacting mixture flowing through the reactor reaches the reaction zone (the zone in which the kinetics of radical decay is recorded and analyzed during the experiment). Numerical kinetic modeling performed without this assumption for the typical conditions of the experiments ([C₃H₃] = 2.39 × 10¹³ molecules cm⁻³, bath gas density 6.0 × 10¹⁶ molecules cm⁻³, [(CClO)₂] = 2.63 × 10¹⁵ molecules cm⁻³, [C₃H₄] = 3.67 × 10¹⁵ molecules cm⁻³) with the rate of thermal production of C₃H₃ fitted to reproduce the observed signal of propargyl radicals before the laser pulse resulted in the value of k_1 that differed from the exact one by only 0.3%. The Kintecus³¹ kinetic modeling program was used in these calculations and in those described below.

A significantly larger effect on the kinetics of reaction 1 at 1000 K could have been caused by the secondary reactions of the phenyl radicals and hydrogen atoms formed in one of the channels of reaction 1. As mentioned above, phenyl radicals are expected to quickly react with the excess of propyne producing stable species (C₈H₆, C₆H₆, and C₉H₈) and radicals (CH₃, H, and C₃H₃). H atoms formed in reaction 1 will also react with propyne, either by abstracting a hydrogen atom and

regenerating C₃H₃ or by adding to the triple bond with subsequent decomposition of the chemically activated adduct into CH₃ and C₂H₂. Overall, the following reactions could participate in the ensuing kinetics:



Accurate modeling of the effects of these secondary reactions is impossible due to lack of reliable experimental information on the values of the rate constants and branching ratios of reactions 1 and 5–7. Theoretical studies of these reactions exist in the literature: reactions 6 and 7 between H atom and propyne have been studied computationally by Wang et al.³² and Davis et al.³³ the reaction between the phenyl radical and propyne has been studied by Vereecken et al.²⁹ However, the reliability of these results is not easily evaluated, which has negative consequences for modeling. In particular, all four channels of reaction 5 are predicted²⁹ to have comparable yields at 1000 K and the pressures used in the experiments of the current study. Thus, it can be expected that even small uncertainties in the values of energy barriers responsible for individual channels of reaction 5 and the associated preexponential factors can result in large uncertainties in the distribution of channels.

Nevertheless, a simplified analysis of uncertainties caused by secondary reactions can be performed. Channels of the secondary reactions of phenyl and H formed in reaction 1 can be divided into two groups: one leading to the formation of methyl radicals (reactions 5a and 7) and the other leading to the regeneration of propargyl radicals (reactions 5d and 6). Reactions of the first group will lead to an increase of the propargyl decay due to reaction 9 and thus to overestimated values of the observed rate constant of reaction 1. Reactions of the second group will lead to underestimation of the value of k_1 . Two limiting cases can be considered. In the first case, the kinetic mechanism favors reactions leading to formation of methyl radical ($k_6 = k_{5d} = 0$; H atoms produced in reactions 1b, 5b, and 5c react with propyne generating CH₃). In the second limiting case, reactions leading to regeneration of the propargyl radical are favored ($k_7 = k_{5a} = 0$, H atoms react with propyne only through abstraction generating C₃H₃).

In the second limiting case, the phenyl radical and the H atom products of the reaction channel 1b will each produce one propargyl radical. Thus, reaction channel 1c will not be observed in the experiments where the decay of C₃H₃ is monitored.

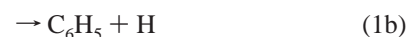
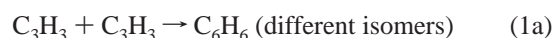
Therefore, the experimental value of k_1 will correspond only to the channel producing C₆H₆, $k_1 = k_{1a}$.

To estimate the effects of secondary chemistry in the first limiting case, numerical kinetic modeling using the above reaction mechanism was performed. The rate constants of reactions 1a and 1b were taken as equal to each other and were adjusted together with the rate of production of C₃H₃ due to the thermal decomposition of oxalyl chloride (reaction 2c) to obtain the C₃H₃ concentration profile that, when fitted with eq I, would produce the experimentally observed values of $k_t[\text{R}]_0$ and k_4 (see sections II and III). Experimental conditions of the particular experiment (representative of the typical conditions) described above in the discussion of the effects of the thermal decomposition of oxalyl chloride were used. The values of k_8 and k_9 under these conditions were calculated using the parametrization of Hessler and Ogren³⁴ ($k_8 = 2.5 \times 10^{-12} \text{ cm}^{-3} \text{ molecule}^{-1} \text{ s}^{-1}$) and the experiment-based model of Knyazev and Slagle³⁵ ($k_9 = 9.3 \times 10^{-12} \text{ cm}^{-3} \text{ molecule}^{-1} \text{ s}^{-1}$). The effect of secondary chemistry was found to be relatively minor, which is explained by the low (due to the high temperature and falloff effects) rate constant of the C₃H₃ + CH₃ reaction. The value of the rate constant of the propargyl radical self-reaction determined from the simulation was found to be only 8% lower than the observed value (Table 1).

The results of the above analysis of the secondary chemistry occurring in the real-time experiments performed at 1000 K demonstrate that the observed value of $k_1(1000 \text{ K}) = (1.20 \pm 0.14) \times 10^{-11} \text{ cm}^{-3} \text{ molecule}^{-1} \text{ s}^{-1}$ is likely to lie between the true values of k_{1a} (the rate constant of the C₆H₆-producing channels of propargyl self-reaction) and $\sim 1.1k_1$ (the overall rate constant of reaction 1 increased by 10%). Future experimental studies of the rate constants and the products of reactions 5, 6, and 7, as well as those of the branching fraction of the phenyl-producing channel of reaction 1, can be expected to reduce the uncertainty bounds of the rate constant of reaction 1 obtained in the current work at 1000 K.

V. Conclusions

The kinetics of the self-reaction of propargyl radicals



has been studied in direct experiments by laser photolysis/photoionization mass spectrometry over the temperature interval 500–1000 K and at the bath gas (mostly helium, balance radical precursors) density of $(3\text{--}6) \times 10^{16} \text{ molecules cm}^{-3}$. Propargyl radicals were produced by the 248 nm laser photolysis of oxalyl chloride ((CClO)₂ → 2Cl + 2CO) followed by the fast conversion of the chlorine atoms into propargyl radicals via the reaction with propyne (Cl + C₃H₄ → C₃H₃ + HCl). Thus, no active species other than C₃H₃ were present in the system during the kinetics of C₃H₃ decay. Initial concentrations of the C₃H₃ radical were determined from the measured (in real time) production of HCl. The kinetics of C₃H₃ decay was monitored in real time, and the values of the rate constant of reaction 1 were determined from the [C₃H₃] temporal profiles.

The obtained values of the rate constant of reaction 1 decrease from $(3.30 \pm 0.35) \times 10^{-11} \text{ cm}^3 \text{ molecule}^{-1} \text{ s}^{-1}$ at 500 K to $(2.74 \pm 0.43) \times 10^{-11} \text{ cm}^3 \text{ molecule}^{-1} \text{ s}^{-1}$ at 700 K and to $(1.20 \pm 0.14) \times 10^{-11} \text{ cm}^3 \text{ molecule}^{-1} \text{ s}^{-1}$ at 1000 K. The value obtained at 1000 K is likely to be influenced by the falloff effects. Kinetics observed at 1000 K was affected by secondary reactions caused by the production of the C₆H₅ + H products

in one of the channels of reaction 1. Analysis of the secondary chemistry demonstrates that the value of the rate constant observed at 1000 K is likely to lie between the true values of k_{1a} (the rate constant of the C_6H_6 -producing channels of propargyl self-reaction) and $\sim 1.1k_1$ (the overall rate constant of reaction 1 increased by 10%).

The rate constants of reaction 1 obtained in the current study correlate well with the room temperature values of Fahr and Nayak $((4.0 \pm 0.4) \times 10^{-11} \text{ cm}^3 \text{ molecule}^{-1} \text{ s}^{-1})$,⁵ Atkinson and Hudgens $((4.3 \pm 0.6) \times 10^{-11} \text{ cm}^3 \text{ molecule}^{-1} \text{ s}^{-1})$,¹¹ and DeSain and Taatjes $((3.9 \pm 0.6) \times 10^{-11} \text{ cm}^3 \text{ molecule}^{-1} \text{ s}^{-1})$.¹³ Combination of the results of the current study with those of earlier room temperature investigations^{5,11,13} results in the following temperature dependence of the high-pressure-limit rate constant over the 295–700 K temperature interval:

$$k_1^\infty = 4.49 \times 10^{-9} T^{-0.75} \exp(-128 \text{ K}/T) \text{ cm}^3 \text{ molecule}^{-1} \text{ s}^{-1} \quad (\text{II})$$

Product channels of reaction 1 were studied using final product analysis by gas chromatography/mass spectrometry in the temperature interval 500–1100 K. Several C_6H_6 isomers were detected as products of the self-reaction of propargyl radicals: 1,5-hexadiyne, fulvene, benzene, and two unknown species identified in the text as unknown 1 and unknown 2. The distribution of products depends on the temperature. At lower temperatures, 1,5-hexadiyne, unknown 1, and benzene were observed. The fraction of benzene increases with temperature; it becomes the major product at 900 K and above. Fulvene and unknown 2 were observed in minor amounts in the 900–1100 K range. The final product analysis provides evidence for the appearance of the reaction channel 1b ($C_6H_5 + H$) at high temperatures: formation of C_8H_6 and C_9H_8 was observed and attributed to the fast reaction of the phenyl radical with the excess of propyne present in the reactor.

Acknowledgment. This research was supported by Division of Chemical Sciences, Office of Basic Energy Sciences, Office of Energy Research, U.S. Department of Energy, under Grant DE/FG02-98ER14463. The authors thank Dr. A. Fahr for sharing with them the ion fragmentation pattern of fulvene obtained in the 2000 study of Fahr and Nayak.

Supporting Information Available: Ion fragmentation patterns observed in the GC/MS analysis of the C_6H_6 isomers obtained from commercial sources, in thermal isomerization

experiments, and in the product study of reaction 1. This material is available free of charge via the Internet at <http://pubs.acs.org>.

References and Notes

- (1) Richter, H.; Howard, J. B. *Prog. Energy Combust. Sci.* **2000**, *26*, 565.
- (2) Wu, C. H.; Kern, K. D. *J. Phys. Chem.* **1987**, *91*, 6291.
- (3) Kern, R. D.; Wu, C. H.; Yong, J. N.; Pamidimukkala, K. M.; Singh, H. J. *Energy Fuels* **1988**, *2*, 454.
- (4) Alkemade, U.; Homann, K. H. Z. *Phys. Chem. (Munich)* **1989**, *161*, 19.
- (5) Fahr, A.; Nayak, A. *Int. J. Chem. Kinet.* **2000**, *32*, 118.
- (6) Stein, S. E.; Walker, J. A.; Suryan, M. M.; Fahr, A. *Proc. Combust. Inst.* **1990**, *23*, 85.
- (7) Miller, J. A.; Melius, C. F. *Combust. Flame* **1992**, *91*, 21.
- (8) Melius, C.; Miller, J. A.; Evleth, E. M. *Proc. Combust. Inst.* **1992**, *24*, 621.
- (9) Slagle, I. R.; Gutman, D. *Proc. Combust. Inst.* **1988**, *21*, 875.
- (10) Morter, C. L. F. S. K.; Adamson, J. D.; Glass, G. P.; Curl, R. F. J. *Phys. Chem.* **1994**, *98*, 7029.
- (11) Atkinson, D. B.; Hudgens, J. W. *J. Phys. Chem. A* **1999**, *103*, 4242.
- (12) Scherer, S.; Just, Th.; Frank, P. *Proc. Combust. Inst.* **2000**, *28*, 1511.
- (13) DeSain, J. D.; Taatjes, C. A. *J. Phys. Chem. A* **2003**, *107*, 4843.
- (14) Giri, B. R.; Hippler, H.; Olzmann, M.; Unterreiner, A. N. *Phys. Chem. Chem. Phys.*, submitted for publication. Preliminary results presented at the 17th International Symposium on Gas Kinetics, Essen, Germany, 2002.
- (15) Howe, P. T.; Fahr, A. *J. Phys. Chem. A*, submitted for publication.
- (16) Miller, J. A.; Klippenstein, S. J. *J. Phys. Chem. A* **2001**, *105*, 7254.
- (17) Miller, J. A.; Klippenstein, S. J. *J. Phys. Chem. A*, in press.
- (18) A preliminary report was presented at the 17th International Symposium on Gas Kinetics, Aug 2002, Essen, Germany.
- (19) Baklanov, A. V.; Krasnoperov, L. N. *J. Phys. Chem. A* **2001**, *105*, 97.
- (20) Baklanov, A. V.; Krasnoperov, L. N. *J. Phys. Chem. A* **2001**, *105*, 4917.
- (21) Farrell, J. T.; Taatjes, C. A. *J. Phys. Chem. A* **1998**, *102*, 4846.
- (22) Slagle, I. R.; Gutman, D. *J. Am. Chem. Soc.* **1985**, *107*, 5342.
- (23) Niiranen, J. T.; Gutman, D.; Krasnoperov, L. N. *J. Phys. Chem.* **1992**, *96*, 5881.
- (24) Shafir, E. V.; Slagle, I. R.; Knyazev, V. D. *J. Phys. Chem. A* **2003**, *107*, 6804.
- (25) Hemmi, N.; Suits, A. G. *J. Phys. Chem. A* **1997**, *101*, 6633.
- (26) Ahmed, M.; Blunt, D.; Chen, D.; Suits, A. G. *J. Chem. Phys.* **1997**, *106*, 7617.
- (27) Nicovich, J. M.; Kreutter, K. D.; Wine, P. H. *J. Chem. Phys.* **1990**, *92*, 3539.
- (28) Slagle, I. R.; Gutman, D.; Davies, J. W.; Pilling, M. J. *J. Phys. Chem.* **1988**, *92*, 2455.
- (29) Vereecken, L.; Bettinger, H.; Peeters, J. *Phys. Chem. Chem. Phys.* **2002**, *4*, 2019.
- (30) Madden, L. K.; Mebel, A. M.; Lin, M. C.; Melius, C. F. *J. Phys. Org. Chem.* **1996**, *9*, 801.
- (31) Ianni, J. C. *Kintecus*, Windows version 2.80, 2002.
- (32) Wang, B.; Hou, H.; Gu, Y. *J. Chem. Phys.* **2000**, *112*, 8458.
- (33) Davis, S. G.; Law, C. K.; Wang, H. *J. Phys. Chem. A* **1999**, *103*, 5889.
- (34) Hessler, J. P.; Ogren, P. J. *J. Phys. Chem.* **1996**, *100*, 984.
- (35) Knyazev, V. D.; Slagle, I. R. *J. Phys. Chem. A* **2001**, *105*, 3196.
- (36) Daly, N. R. *Rev. Sci. Instrum.* **1960**, *31*, 264.